Quantitative deformation analysis differentiates ischaemic and non-ischaemic cardiomyopathy: sub-group analysis of the VINDICATE trial

Dr James RJ Foley BSc Hons MBChB   j.foley@leeds.ac.uk

Dr Peter P Swoboda PhD   p.swoboda@leeds.ac.uk

Dr Graham J Fent BSc Hons MBChB   g.j.fent@leeds.ac.uk

Dr Pankaj Garg MD   p.garg@leeds.ac.uk

Dr Adam K. McDiarmid MD   a.k.mcdiarmid@leeds.ac.uk

Dr David P Ripley MBChB   d.ripley@leeds.ac.uk

Dr Bara Erhayiem MBBS   b.erhayeim@leeds.ac.uk

Dr Tarique Al Musa PhD   t.a.musa@leeds.ac.uk

Dr Laura E Dobson MD   l.dobson@leeds.ac.uk

Prof. Sven Plein MD, PhD   s.plein@leeds.ac.uk

Dr Klaus K Witte MD   k.k.witte@leeds.ac.uk

Prof. John P Greenwood MBChB, PhD   j.greenwood@leeds.ac.uk

Word count (including references and figure legends and tables)**: 4931**

Multidisciplinary Cardiovascular Research Centre (MCRC) & Leeds Institute of Cardiovascular and Metabolic Medicine, University of Leeds, Clarendon Way, Leeds, LS2 9JT, UK

Address for correspondence:

Prof. John Greenwood,

Multidisciplinary Cardiovascular Research Centre & Division of Biomedical Imaging,

Leeds Institute of Cardiovascular and Metabolic Medicine,

University of Leeds,

Leeds, LS2 9JT

Tel +44 113 3925398

Fax +44 113 3926022

E-mail: j.greenwood@leeds.ac.uk

Abstract

Aims

To test the hypothesis that patients with ischaemic cardiomyopathy (ICM) and non-ischaemic cardiomyopathy (NICM) have different torsion and strain parameters, and compare to healthy, age matched controls.

VINDICATE investigated efficacy of high-dose vitamin D on patients with heart failure (HF) secondary to left ventricular (LV) systolic dysfunction of any aetiology. It is important to differentiate ICM and NICM as treatment and prognosis varies significantly. CMR reliably determines aetiology of HF and tissue tagging techniques are recognised as the reference standard measures of strain and torsion.

Methods and Results

53 patients (31 ICM, 22 NICM) from VINDICATE and 25 controls underwent CMR at 3.0T, including cine imaging in multiple planes and tissue tagging by spatial modulation of magnetization. CMR data were analysed blinded, by quantitatively reporting circumferential strain and torsion from tagged images and global longitudinal strain from feature tracking.

HF patients had larger ventricles indexed to BSA, lower LVEF, LV torsion, twist, and strain parameters compared to controls.

There were no significant differences between ICM and NICM in age, blood pressure, heart rhythm or NYHA status.

There was no significant difference in LV dimensions, EF and strain parameters between ICM and NICM. NICM patients had significantly lower LV twist (6.0 ± 3.7^{o} vs. 8.8 ± 4.3^{o}, p=0.023) and torsion (5.9 ± 3.5^{o} vs. 8.8 ± 4.7^{o}, p=0.017) compared to ICM.

Conclusions

Twist, torsion and strain are reduced in HF patients compared to controls. Torsion and twist are significantly lower in patients with NICM compared to ICM, despite similar volumetric dimensions, circumferential and longitudinal strain parameters and LVEF.

Key words (6)

Cardiovascular magnetic resonance; tagging; feature tracking; heart failure; left ventricular function

Introduction

Heart failure with reduced ejection fraction (HFrEF) is caused by a diverse range of pathologies that contribute to the overall syndrome [1–3]. Identification of the aetiology of cardiomyopathy provides both insights into the pathophysiology, as well as directing specific therapeutic interventions, whilst conferring prognostic information [2,3]. Ischaemic (ICM) and non-ischaemic cardiomyopathy (NICM) can manifest extremely similar phenotypes, though management may be divergent and consequently current guidelines suggest clarification of the aetiology for this reason [2,3]. Multi-parametric cardiovascular magnetic resonance (CMR) can help to distinguish these aetiologies [3]. Strain, twist and torsion are measures of myocardial performance beyond ejection fraction. Strain is an index of deformation from the initial to maximal length of a myocardial segment (%) [4]. Twist (°) describes the relative rotation between the apex and base of the ventricle (peak difference between systolic rotation of LV apex and base viewed from the apex/). Torsion (°) describes the complex "wringing" motion of the left ventricle that is influenced by of both the twisting motion of the heart and size of the ventricular cavity [5]. The torsional shear angle (°) is calculated by measuring the radius of the apical and basal slices multiplied by the twist and divided by the distance between them [6]. In the normal heart the base of the ventricle rotates clockwise during systole whilst the apex rotates counter clockwise [6]. Left ventricular torsion is a primary component of normal systolic function and has been identified as a sensitive marker for transplant rejection, myocardial ischaemia and infarction, successful ventricular reconstruction surgery as well as a predictor of responsiveness to cardiac resynchronisation therapy [7–12]. These parameters can be quantified by CMR tissue tagging techniques, which are highly reproducible and recognised as the reference standard non-invasive measures of myocardial strain and torsion [8,13–16].

The VINDICATE (VitamIN D treatIng patients with Chronic heArT failurE) study was a randomised placebo-controlled double-blind trial designed to describe the safety and efficacy of long-term, high-dose vitamin D_3 supplementation on submaximal exercise capacity and cardiac function in vitamin D−deficient patients with chronic heart failure (HF) due to left ventricular systolic dysfunction already established on optimal medical therapy [17]. A subgroup of the study underwent additional investigation using multi-parametric CMR. In this sub-study we investigated the relationship between strain-derived parameters and aetiology of HFrEF and hypothesised that in a prospectively recruited random sample of HFrEF patients ICM and NICM would have distinctive myocardial torsion patterns.

Methods

Study participants

The inclusion criteria for VINDICATE have been previously reported [17]. In summary, all patients had stable (>3 months) New York Heart Association (NYHA) functional class II or III symptoms, a left ventricular ejection fraction (LVEF) ≤45% on maximally tolerated medical therapy (>3 months) and a 25(OH) vitamin D level of <50 nmol/l (<20 ng/ml). Patients were invited to enter the CMR substudy at their initial enrolment visit. Exclusion criteria included history of taking calcium or other vitamin supplements in the preceding 3 months; aetiology of chronic HF due to untreated valvular heart disease, anaemia or thyrotoxicosis; existing indications for vitamin D supplementation; history of primary hyperparathyroidism, sarcoidosis, tuberculosis or lymphoma; cholecalciferol concentration >50 nmol/l (20 ng/ml); or if there was significant renal dysfunction (estimated glomerular filtration rate <30 ml/min/1.73m^2)[17]. Aetiology of heart failure was determined by the enrolling clinician. ICM was defined as left ventricular dysfunction associated with previous significant coronary disease (>70% in at least one major epicardial coronary artery) on angiography, positive ischaemia testing with SPECT or stress echocardiography and/or history of previous myocardial infarction or revascularisation [17]; NICM was defined as left ventricular dysfunction in the absence of the previous conditions. A control group of age-matched volunteers with no significant co-morbidities were enrolled and underwent an identical CMR protocol.

The study was performed in accordance with the Declaration of Helsinki, with all patients providing informed written consent. The study protocol and other relevant documentation had been approved by the National Research Ethics Service [12/YH/0206]; VINDICATE was funded by the Medical Research Council, UK.

Cardiac Magnetic Resonance Protocol

CMR was performed on a 3 Tesla Philips Achieva system (Philips Healthcare, Best, The Netherlands) equipped with a 32 channel coil and MultiTransmit® technology. Data was acquired at end expiration during breath-holding. Cine images were acquired covering the entire heart in the LV short axis plane (balanced steady state free precession), spatial resolution 1.2x1.2x10mm³, 30 cardiac phases TR/TE 2.6/1.3ms, flip angle 40º, field of view 300-420mm, typical temporal resolution 39ms) and in orthogonal long-axis planes. Tissue tagging by spatial modulation of magnetization (spatial resolution $1.51x1.57x10mm^3$, tag separation 7 mm, ≥18 phases, typical TR/TE 5.8/3.5ms, flip angle 10º, typical temporal resolution 55ms) was acquired in three short axis slices at the apex, mid-ventricle, and base. Consistent slice positioning was performed according to the widely accepted "3 of 5 technique" [18]. Late gadolinium enhancement imaging was undertaken 15 minutes following administration of 0.15mmol/kg gadolinium DTPA (Gadovist, Bayer Schering) using an inversion recovery-prepared T1-weighted gradient echo pulse sequence. Selection of the appropriate inversion time (TI) to null normal myocardial signal was ascertained by the Look-Locker approach. Between 10 and 12 short axis slices and, 2 chamber and 4 chamber images were acquired for each participant.

Image Analysis

CMR data were analysed quantitatively using commercially available software (CVI42, Circle Cardiovascular Imaging Inc. Calgary, Canada and inTag v1.0, CREATIS lab, Lyon, France). Endocardial borders were traced on the LV cine stack at end-diastole and end-systole to calculate end diastolic volume, end systolic volume (ESV), stroke volume (SV) and ejection fraction (EF). Contours were traced to exclude papillary muscles and trabeculations. Volumetric data were indexed to body surface area calculated by the Mosteller equation. Late

gadolinium enhancement was assessed quantitatively using the semi-automated full width half maximum method.

For tagging analysis, endocardial and epicardial contours were drawn on the short axis spatial modulation of magnetization images using a semi-automated process. Peak circumferential LV strain was measured for the three slices at apex, mid-ventricle, and base. Strain was measured in the mid-myocardial layer which has previously been reported to be the most reproducible [13]. LV twist was calculated by subtracting the basal from apical rotation. Basal and apical radius was calculated from cine images in diastole at the same slice location as the tagged images. The equation used to determine torsion was [6]:

$$Torsion = \frac{Peak\ Twist\ \times (Apical\ Radius + Basal\ Radius)}{2\ \times Apex\ to\ Base\ length}$$

Feature tracking rather than spatial modulation of magnetization was used for the analysis of global longitudinal strain. For this, endocardial and epicardial contours were drawn on 4 chamber cine images using a semi-automated process and peak longitudinal strain and systolic strain rate were measured for the LV.

Statistical Analysis

Statistical analysis was performed using IBM SPSS® Statistics 20.0 (IBM Corp., Armonk, NY). Continuous variables were expressed as means ± SD. Categorical variables were expressed as N (%). Normality of data was tested using a Shapiro-Wilk test. Unpaired Student t-test and Mann-Whitney were used as appropriate to compare continuous variables. Chi-square test was used for categorical data. P<0.05 was considered statistically significant.

Results

223 patients were enrolled in VINDICATE, but as CMR was not mandated in the clinical trial protocol, only a subgroup of 69 patients underwent a baseline CMR scan. Of these 53 had myocardial tagging sequences performed and were included in this analysis. 25 age-matched

controls with no co-morbidity and taking no regular medication underwent an identical CMR scan. Table 1 shows the demographic data for the combined HF group and controls. There were no significant differences between age, height, weight and BMI. Table 2 shows the CMR imaging characteristics and strain parameters of both the HF and control groups. Compared with controls, patients with HF had significantly larger ventricles when indexed to body surface area and significantly lower values of LVEF, LV torsion and twist, circumferential and longitudinal strain.

Table 3 shows the baseline demographics between the ICM and NICM patients. There were no significant differences between groups in terms of age, blood pressure, heart rhythm or baseline NYHA status. ICM patients had undergone significantly more prior revascularisation (PCI, CABG) than NICM patients. Table 4 shows CMR volumetric data and functional parameters between the ICM and NICM patients. There was no significant difference in LV dimensions, LV mass and EF between the two groups. ICM patients had significantly more infarct pattern late gadolinium enhancement than NICM (77% vs. 0% p<0.001). Mean percentage of infarction was 19.0±7.6% in the ICM group. Three patients in the NICM group had mid wall pattern late enhancement, no other late enhancement patterns were seen in this group. Strain parameters showed no differences in circumferential strain at any short axis level or in terms of global longitudinal strain between the two groups. NICM patients had significantly lower LV twist (6.0±3.7º vs. 8.8±4.3º, p=0.023) (figure 1) and torsion (5.9±3.5º vs. 8.8±4.7º, p=0.017) compared to the ICM group. There was no significant correlation of twist (r= -0.113 P=0.424) or torsion (r= -0.096 P=0.4938) with patient functional assessment measures from a standard six minute walk test.

In patients with ICM and no late gadolinium enhancement (n=7), again there were no significant differences compared to NICM patients in CMR volumetric data (LVEDVi 95.5±15.4ml/m^2 vs. 115.3±48.5ml/m^2 p=0.272) or LVEF (40.9±12.2% vs. 36.0±11.7%

p=0.332). Furthermore, there were no significant differences between these groups in any strain parameters (E_{cc}Apex 10.7±7.6% vs. 10.9±7.4% p=0.947, E_{cc}Mid 11.8±9.3% vs. 10.7±6.6% p=0.721, E_{cc}Base 8.0±7.3% vs. 11.4±4.8% p=0.168, GLS 12.6±3.5% vs. 11.3±7.5% p=0.627). Notably, there was no significant difference in twist or torsion between the ICM patients without late gadolinium enhancement and the NICM patients (twist 9.6±4.9° vs. 6.0±3.7° p=0.051, torsion 7.9±5.6° vs. 5.9±3.5° p=0.248).

Discussion

We have shown that all myocardial mechanical parameters including strain, twist and torsion were reduced in HF patients compared to age-matched controls. More importantly, despite having similar left ventricular dimensions, EF and strain parameters, patients with NICM have significantly less LV twist and torsion than patients with ICM.

Thus far there have been no comparisons of LV mechanics performed between different aetiologies of HFrEF. Our study identified a significant difference between LV torsion and twist in patients with different aetiologies of heart failure. Torsion and strain are currently not routinely measured during CMR imaging for cardiomyopathy, although CMR is the reference standard for these measurements and it is increasingly recommended to guide management [3]. Our study shows that measurements of LV strain and torsion parameters measured by CMR can give potential mechanistic insights into the aetiology and pathophysiology of LV dysfunction. Prognostic benefit is seen with therapeutic interventions according to aetiology [19] and thus accurate delineation of aetiology becomes paramount [3].

Left ventricular torsion has been proposed as a mechanism to reduce myocardial fibre strain in order to improve energy efficiency and decrease oxygen demand [20,21], whilst untwisting contributes to the diastolic function of the ventricle during isovolumetric relaxation [6]. Torsion can be influenced by different loading conditions such as hypertension, athletic training and alters with increasing age [6,22]. LV torsion results as a consequence of the fibrous architecture of the heart (figure 1). Subepicardial fibres of the ventricle are arranged helically in a right handed oblique orientation of around 60°, whilst subendocardial fibres run in an opposing left handed helix of around 80° [5,6,23]. This opposing arrangement of fibres results in shear deformation, with the predominant direction of force occurring in a clockwise direction as a result of the greater rotational radius of the subepicardial layer [20,24].

In patients with ischaemic heart disease, the wave-front of myocardial ischaemia first affects subendocardial fibres prior to the subepicardial layer, with a similar effect on myocardial contraction patterns [25]. In dog models of infarction, endocardial fibres show loss of tissue and function, while epicardial fibres demonstrate functional recovery, likely as a result of early reperfusion [26,27]. Correspondingly in man, Wu et al demonstrated by diffusion tensor MRI [28], subendocardial right handed fibres reduced following infarction whilst the percentage of left handed fibres in the subepicardium increased, potentially as a result of a compensatory remodelling process [28]. These structural changes are reflected in imaging studies of LV mechanics that show, according to the degree of transmurality of infarction, that subendocardial function is similarly reduced in both small and large STEMI, whilst subepicardial fibre function is reduced only in large STEMI (full thickness infarction) and is severely reduced in those with chronic ischaemic HF (the latter finding corresponding with the lack of significant difference seen in twist and torsion between the chronically ICM without scar and NICM) [9,29,30].

ICM tends to show regional dysfunction compared to NICM that shows more global myocardial fibre dysfunction [1]. Torsion and twist have both been shown to be reduced in a variety of NICM [31–33]. NICM can result in a variety of altered contraction patterns including a global reduction in torsion [34]; paradoxical reversal of LV rotation with the base rotating counter clockwise and the apex rotating clockwise [35]; and in some cases both apical and basal segments rotate in the same direction leading to "rigid body rotation" where the wringing motion of the ventricle is lost altogether [33]. Furthermore a reduction in LV torsion is noted in tandem with the degree of spherical LV remodelling [31]. These findings are consistent with our study that shows that patients with cardiomyopathy have a reduction of torsion compared to healthy controls, but also that patients with NICM have reduced torsion relative to ICM. The relative preservation of LV torsion in ICM compared to NICM (8.8±4.7º vs. 5.9±3.5º p=0.017) seen in

our study is explained by the differential effect on subepicardial fibres by necrosis and ischaemia in ICM with some regions spared, contrary to the global myocyte dysfunction seen in NICM. Furthermore it has been hypothesised that remaining subepicardial fibres in ICM undergo hypertrophy and recruitment as an active remodelling process following ischaemic insults thus contributing to the higher torsion values seen in ICM compared to NICM [27,28].

Strain is a measure of myocardial deformation and has been proposed as being more sensitive to changes in LV mechanics than ejection fraction and is influenced by compensatory changes such as ventricular dilatation or geometrical change [4]. Furthermore global longitudinal strain has been identified as a marker of prognosis over and above ejection fraction in a variety of conditions [36,37]. In our study, neither EF nor strain parameters were significantly different between cardiomyopathy of either aetiology. GLS is predominantly a result of subendocardial longitudinal fibres, whilst circumferential strain is attributed to the radial fibres that are distributed in the mid-wall of the ventricle and the subepicardial fibres [5, 23,37–39]. These fibres in, or adjacent to, the subepicardium are affected by ischaemia prior to the subepicardial fibres and thus intuitively circumferential and longitudinal strain are reduced greater than LV torsion in ICM, whilst leading to the similar strain values seen in patients with NICM.

Limitations

Our observational study has a number of limitations. The sample size is relatively small and differences in baseline demographics, comorbidities and treatment may be a potential source of bias. However both cardiomyopathy groups and controls were prospectively enrolled, and were age-matched, which is an important consideration as age has been shown to affect strain, torsion and twist [40]. Through plane motion is a limitation of using 2D tagging methods. This may have an effect due to the global deformation changes seen in NICM versus local changes

in contractile properties in ICM. The 2D method used in our paper has consistently been shown to be reliable and reproducible in a variety of patient groups[13, 22,41,42], and 2D and 3D tagging methods for LV torsion have been shown to strongly related [43]. Currently 3D methods of CMR tagging are time consuming requiring multiple breath holds of long duration [44,45], thus from a pragmatic point of view we used a reproducible 2D method that required a single breath hold per slice that in general HF patients would be able to tolerate. Estimation of diffuse fibrosis by T1 mapping and ECV calculation were not performed in this study, which may have provided further insight.

Conclusion

Twist, torsion and strain are reduced in patients with cardiomyopathy compared to controls. Torsion and twist are significantly lower in patients with NICM compared to ICM, despite similar volumetric dimensions, circumferential and longitudinal strain parameters and LVEF.

Acknowledgements

References

1. Braunwald E. Heart failure. JACC Heart Fail 2013;**1**:1–20.

2. Yancy CW, Jessup M, Bozkurt B, Butler J, Casey DE, Drazner MH, et al. 2013 ACCF/AHA guideline for the management of heart failure: a report of the American College of Cardiology Foundation/American Heart Association Task Force on Practice Guidelines. J Am Coll Cardiol 2013;**62**:e147-239.

3. Ponikowski P, Voors AA, Anker SD, Bueno H, Cleland JGF, Coats AJS, et al. 2016 ESC Guidelines for the diagnosis and treatment of acute and chronic heart failure: The Task Force for the diagnosis and treatment of acute and chronic heart failure of the European Society of Cardiology (ESC). Developed with the special contribution . Eur J Heart Fail 2016;**18**:891–975.

4. D'Elia N, D'hooge J, Marwick TH. Association Between Myocardial Mechanics and Ischemic LV Remodeling. JACC Cardiovasc Imaging 2015;**8**:1430–1443.

5. Streeter DD, Spotnitz HM, Patel DP, Ross J, Sonnenblick EH. Fiber orientation in the canine left ventricle during diastole and systole. Circ Res 1969;**24**:339–347.

6. Young AA, Cowan BR. Evaluation of left ventricular torsion by cardiovascular magnetic resonance. J Cardiovasc Magn Reson 2012;**14**:49.

7. Hansen DE, Daughters GT, Alderman EL, Stinson EB, Baldwin JC, Miller DC. Effect of acute human cardiac allograft rejection on left ventricular systolic torsion and diastolic recoil measured by intramyocardial markers. Circulation 1987;**76**:998–1008.

8. Buchalter MB, Rademakers FE, Weiss JL, Rogers WJ, Weisfeldt ML, Shapiro EP. Rotational deformation of the canine left ventricle measured by magnetic resonance tagging: effects of catecholamines, ischaemia, and pacing. Cardiovasc Res 1994;**28**:629–635.

9. Bertini M, Delgado V, Nucifora G, Ajmone Marsan N, Ng ACT, Shanks M, et al. Left

ventricular rotational mechanics in patients with coronary artery disease: differences in subendocardial and subepicardial layers. Heart 2010;**96**:1737–1743.

10. Paetsch I, Föll D, Kaluza A, Luechinger R, Stuber M, Bornstedt A, et al. Magnetic resonance stress tagging in ischemic heart disease. Am J Physiol Heart Circ Physiol 2005;**288**:H2708-14.

11. Setser RM, Smedira NG, Lieber ML, Sabo ED, White RD. Left ventricular torsional mechanics after left ventricular reconstruction surgery for ischemic cardiomyopathy. J Thorac Cardiovasc Surg 2007;**134**:888–896.

12. Sade LE, Demir Ö, Atar I, Müderrisoglu H, Özin B. Effect of Mechanical Dyssynchrony and Cardiac Resynchronization Therapy on Left Ventricular Rotational Mechanics. Am J Cardiol 2008;**101**:1163–1169.

13. Swoboda PP, Larghat A, Zaman A, Fairbairn TA, Motwani M, Greenwood JP, et al. Reproducibility of myocardial strain and left ventricular twist measured using complementary spatial modulation of magnetization. J Magn Reson Imaging 2014;**39**:887–894.

14. Young AA, Axel L, Dougherty L, Bogen DK, Parenteau CS. Validation of tagging with MR imaging to estimate material deformation. Radiology 1993;**188**:101–108.

15. Rüssel IK, Götte MJW, Bronzwaer JG, Knaapen P, Paulus WJ, Rossum AC van. Left Ventricular Torsion. An Expanding Role in the Analysis of Myocardial Dysfunction. JACC Cardiovasc Imaging 2009;**2**:648–655.

16. Yeon SB, Reichek N, Tallant BA, Lima JAC, Calhoun LP, Clark NR, et al. Validation of in vivo myocardial strain measurement by magnetic resonance tagging with sonomicrometry. J Am Coll Cardiol 2001;**38**:555–561.

17. Witte KK, Byrom R, Gierula J, Paton MF, Jamil HA, Lowry JE, et al. Effects of Vitamin D on Cardiac Function in Patients With Chronic HF. J Am Coll Cardiol 2016;**67**:2593–

2603.

18. Messroghli DR, Bainbridge GJ, Alfakih K, Jones TR, Plein S, Ridgway JP, et al. Assessment of regional left ventricular function: Accuracy and reproducibility of positioning standard short-axis sections in cardiac MR imaging. Radiology 2005;**235**:229–236.

19. Velazquez EJ, Lee KL, Jones RH, Al-Khalidi HR, Hill JA, Panza JA, et al. Coronary-Artery Bypass Surgery in Patients with Ischemic Cardiomyopathy. N Engl J Med 2016;**374**:1511–1520.

20. Arts T, Reneman RS, Veenstra PC. A model of the mechanics of the left ventricle. Ann Biomed Eng 1979;**7**:299–318.

21. Beyar R, Sideman S. Left ventricular mechanics related to the local distribution of oxygen demand throughout the wall. Circ Res 1986;**58**:664–677.

22. Swoboda PP, Erhayiem B, McDiarmid AK, Lancaster RE, Lyall GK, Dobson LE, et al. Relationship between cardiac deformation parameters measured by cardiovascular magnetic resonance and aerobic fitness in endurance athletes. J Cardiovasc Magn Reson 2016;**18**:48.

23. Greenbaum RA, Ho SY, Gibson DG, Becker AE, Anderson RH. Left ventricular fibre architecture in man. Heart 1981;**45**:248–263.

24. Lorenz CH, Pastorek JS, Bundy JM. Delineation of normal human left ventricular twist throughout systole by tagged cine magnetic resonance imaging. J Cardiovasc Magn Reson 2000;**2**:97–108.

25. Reimer KA, Jennings RB. The 'wavefront phenomenon' of myocardial ischemic cell death. II. Transmural progression of necrosis within the framework of ischemic bed size (myocardium at risk) and collateral flow. Lab Invest 1979;**40**:633–644.

26. Ono S, Waldman LK, Yamashita H, Covell JW, Ross J. Effect of coronary artery

reperfusion on transmural myocardial remodeling in dogs. Circulation 1995;**91**:1143–1153.

27.   Homans DC, Pavek T, Laxson DD, Bache RJ. Recovery of transmural and subepicardial wall thickening after subendocardial infarction. J Am Coll Cardiol 1994;**24**:1109–1116.

28.   Wu MT, Tseng WYI, Su MYM, Liu CP, Chiou KR, Wedeen VJ, et al. Diffusion tensor magnetic resonance imaging mapping the fiber architecture remodeling in human myocardium after infarction: Correlation with viability and wall motion. Circulation 2006;**114**:1036–1045.

29.   Abate E, Hoogslag GE, Leong DP, Bertini M, Antoni ML, Nucifora G, et al. Association between multilayer left ventricular rotational mechanics and the development of left ventricular remodeling after acute myocardial infarction. J Am Soc Echocardiogr 2014;**27**:239–248.

30.   Becker M, Ocklenburg C, Altiok E, Füting A, Balzer J, Krombach G, et al. Impact of infarct transmurality on layer-specific impairment of myocardial function: a myocardial deformation imaging study. Eur Heart J 2009;**30**:1467–1476.

31.   Karaahmet T, Gürel E, Tigen K, Güler A, Dündar C, Fotbolcu H, et al. The effect of myocardial fibrosis on left ventricular torsion and twist in patients with non-ischemic dilated cardiomyopathy. Cardiol J 2013;**20**:276–286.

32.   Sengupta PP, Krishnamoorthy VK, Abhayaratna WP, Korinek J, Belohlavek M, Sundt TM, et al. Disparate Patterns of Left Ventricular Mechanics Differentiate Constrictive Pericarditis From Restrictive Cardiomyopathy. JACC Cardiovasc Imaging 2008;**1**:29–38.

33.   Dalen BM van, Caliskan K, Soliman OII, Nemes A, Vletter WB, Cate FJ Ten, et al. Left ventricular solid body rotation in non-compaction cardiomyopathy: a potential new objective and quantitative functional diagnostic criterion? Eur J Heart Fail

2008;**10**:1088–1093.

34. Kanzaki H, Nakatani S, Yamada N, Urayama SI, Miyatake K, Kitakaze M. Impaired Systolic torsion in dilated cardiomyopathy: Reversal of apical rotation at mid-systole characterized with magnetic resonance tagging method. Basic Res Cardiol 2006;**101**:465–470.

35. Meluzin J, Spinarova L, Hude P, Krejci J, Poloczkova H, Podrouzkova H, et al. Left ventricular mechanics in idiopathic dilated cardiomyopathy: systolic-diastolic coupling and torsion. J Am Soc Echocardiogr 2009;**22**:486–493.

36. Antoni ML, Mollema SA, Delgado V, Atary JZ, Borleffs CJW, Boersma E, et al. Prognostic importance of strain and strain rate after acute myocardial infarction. Eur Heart J 2010;**31**:1640–1647.

37. Mignot A, Donal E, Zaroui A, Reant P, Salem A, Hamon C, et al. Global longitudinal strain as a major predictor of cardiac events in patients with depressed left ventricular function: A multicenter study. J Am Soc Echocardiogr 2010;**23**:1019–1024.

38. Garg P, Kidambi A, Foley JRJ, Musa T Al, Ripley DP, Swoboda PP, et al. Ventricular longitudinal function is associated with microvascular obstruction and intramyocardial haemorrhage. Open Hear 2016;**3**:e000337.

39. Rademakers FE, Rogers WJ, Guier WH, Hutchins GM, Siu CO, Weisfeldt ML, et al. Relation of regional cross-fiber shortening to wall thickening in the intact heart. Three-dimensional strain analysis by NMR tagging. Circulation 1994;**89**:1174–1182.

40. Lumens J. Impaired subendocardial contractile myofiber function in asymptomatic aged humans, as detected using MRI. AJP Hear Circ Physiol 2006;**291**:H1573–H1579.

41. Larghat AM, Swoboda PP, Biglands JD, Kearney MT, Greenwood JP, Plein S. The microvascular effects of insulin resistance and diabetes on cardiac structure, function, and perfusion: a cardiovascular magnetic resonance study. Eur Heart J Cardiovasc

Imaging 2014;**15**:1368–1376.

42.   Musa T Al, Uddin A, Swoboda PP, Fairbairn TA, Dobson LE, Singh A, et al. Cardiovascular magnetic resonance evaluation of symptomatic severe aortic stenosis: association of circumferential myocardial strain and mortality. J Cardiovasc Magn Reson Journal of Cardiovascular Magnetic Resonance; 2017;**19**:1–10.

43.   Rüssel IK, Tecelão SR, Kuijer JPA, Heethaar RM, Marcus JT. Comparison of 2D and 3D calculation of left ventricular torsion as circumferential-longitudinal shear angle using cardiovascular magnetic resonance tagging. J Cardiovasc Magn Reson 2009;**11**:8.

44.   Rutz AK, Ryf S, Plein S, Boesiger P, Kozerke S. Accelerated whole-heart 3D CSPAMM for myocardial motion quantification. Magn Reson Med 2008;**59**:755–763.

45.   Stoeck CT, Manka R, Boesiger P, Kozerke S. Undersampled Cine 3D tagging for rapid assessment of cardiac motion. J Cardiovasc Magn Reson 2012;**14**:60.

Figures Legends:

Figure 1.

Tagged images in inTag© analysis. Images A shows apical systolic anticlockwise rotation (red) and B clockwise basal rotation (blue) in a healthy control. Images C shows reduced apical (yellow/red) and D basal (yellow/green) rotation in a patient with ischaemic cardiomyopathy. Images E shows markedly reduced apical (yellow/green) and F basal rotation (yellow/green blue) in a patient with non-ischaemic cardiomyopathy.

Figure 2.

Plots showing apical (blue) and basal (orange) rotation and twist (green) of individual patients with ischaemic and non-ischaemic cardiomyopathy respectively.

Figure 3. Schematic image of LV torsion in normal, ischaemic and non-ischaemic cardiomyopathy (Central Illustration)

Image A shows the subepicardial fibres in red lines that are predominantly responsible for LV torsion. Dotted red lines represent subendocardial fibres arrayed in an opposing helix. The blue arrows show the predominant direction of twist with the base of the ventricle rotating clockwise during systole whilst the apex rotating counter clockwise

Image B shows ischaemic cardiomyopathy, with infarction/ischaemia in black typically affecting subendocardial fibres (yellow) and radial fibres (blue) with preferential sparing of the subepicardial fibres. Torsion is reduced (blue arrows) compared to normal due to some subepicardial fibres being affected.

Image C shows non-ischaemic cardiomyopathy with global myocardial fibre dysfunction leading to significant reduction in torsion due to the effect on subepicardial fibres.

Table 1. Demographic details for HF and healthy control group

	HF group (53)	Controls (25)	P-value
Age, years	62.6±16.4	58.0±12.2	0.164
Sex (female)	17 (32.1)	7 (28)	0.716
Height, cm	170.1±7.8	172.9±12.6	0.389
Weight, kg	78.9±15.1	80.2±18.6	0.762
Body Mass Index, kg/m^2	27.2±4.7	26.6±3.3	0.527
Systolic Blood Pressure, mmHg	117.3±19.8	127.7±14.6	0.026
Diastolic Blood Pressure, mmHg	70.8±10.9	70.2±12.1	0.828
Diabetes Mellitus, %	7 (13)	0	0.122
CABG, %	10 (18.9)	0	0.020
PCI, %	17 (32.1)	0	0.001
AF, %	34 (64.2)	0	<0.001
COPD, %	2 (3.8)	0	0.325

Data as mean ± SD or n (%). AF, atrial fibrillation. CABG, coronary artery bypass grafting.

COPD, chronic obstructive pulmonary disease. PCI, percutaneous coronary intervention.

Table 2. CMR data for HF group and controls

	HF (53)	Controls (25)	P-value
LVEDV, ml	210.5±85.4	160.0±44.7	0.007
LVEDVi, ml/m^2	109.2±38.9	82.2±19.9	<0.001
LVESV, ml	141.6±81.8	68.6±25.3	<0.001
LVEF, %	35.5±10.9	57.6±7.0	<0.001
LGE, (%)	26 (49.0)	0	<0.001
LV twist, º	7.6±4.3	14.6±4.2	<0.001
LV torsion, º	7.6±4.5	13.4±3.1	<0.001
E_{cc} Apex, %	10.4±6.8	22.2±5.3	<0.001
E_{cc} Mid, %	10.4±6.6	21.7± 2.3	<0.001
E_{cc} Base, %	9.6±6.2	20.5±2.6	<0.001
LV longitudinal strain, %	11.0 ±7.3	18.4±2.2	<0.001
LV longitudinal strain rate, %/s	56.5±39.9	93.7±15.9	<0.001

Data as mean ± SD or n (%). $E_{cc,}$ Circumferential strain. LVEDV, left ventricular end diastolic volume. LVEDVi, left ventricular end diastolic volume indexed to body surface area. LVEF, left ventricle ejection fraction. LVESV, left ventricular end systolic volume.

Table 3. Baseline demographics for ischaemic and non-ischaemic cardiomyopathy patients

	ICM (31)	NICM (22)	P-value
Age, years	65.2±15.9	59.0±16.9	0.182
Sex (female)	9, 29%	8, 36%	0.573
Height, cm	170.1±8.1	170.0±7.4	0.970
Weight, kg	78.5±14.2	79.7±16.6	0.773
Body Mass Index, kg/m^2	26.9±3.9	27.6±5.6	0.654
Systolic Blood Pressure, mmHg	119±21	115±18	0.399
Diastolic Blood Pressure, mmHg	70±11	72±11	0.601
Heart rate, bpm	69.2±10.8	69.6±9.5	0.903
Diabetes Mellitus, %	6 (19)	1 (4.5)	0.117
COPD, %	1 (3.2)	1 (4.54)	0.804
CABG, %	10 (32)	0 (0)	0.03
PCI, %	17 (55)	0 (0)	<0.001
AF, %	20 (65)	14 (64)	0.948
BNP, pg/mL	1084±1196	1118±1172	0.421
VO2max, mlO$_2$/min/kg	16.8±5.0	19.7±7.7	0.162
NYHA class II, %	30 (96.8)	22 (100)	0.395

NYHA class III, %	1 (4)	0 (0)	0.395
Beta blockers, %	29 (93.5)	19 (86.4)	0.378
ACEi/ARB, %	28 (90.3)	22 (100)	0.133
Aldosterone antagonist, %	17 (54.8)	11 (50)	0.728
Creatinine, μmol/l	87.5±20.9	80.4±20.6	0.227

Data as mean ± SD or n (%). AF, atrial fibrillation. ACEi, angiotensin-converting enzyme inhibitor. ARB, aldosterone receptor blocker. BNP, natriuretic peptide. CABG, coronary artery bypass grafts. COPD, chronic obstructive pulmonary disease. NYHA, New York Heart Association functional class. PCI, percutaneous coronary intervention.

Table 4. CMR characteristics for ischaemic and non-ischaemic cardiomyopathy patients

	ICM	NICM	P-value
LVEDV, ml	199.4±56.7	226±113.9	0.317
LVEDVi, ml/m^2	104.9±30.5	115.3±48.5	0.343
LVESV, ml	132.8±56.0	153.9±108.8	0.359
LVEF, %	35.1±10.6	36.0±11.7	0.767
LVM, g	134.9±42.6	141.8±70.1	0.655
LVMi, g/m^2	70.4±20.9	72.2±28.9	0.795
LVM/EDV g/ml	0.7±0.3	0.7±0.2	0.378
LGE infarct pattern, %	24. 77.4%	0. 0%	<0.001
LGE mid wall pattern, %	0. 0%	2. 9.0%	0.162
LGE, % of myocardial mass	19.0±7.6%	1.4±4.5	<0.001
LV twist, $^{\circ}$	8.8±4.3	6.0±3.7	0.023
LV torsion, $^{\circ}$	8.8±4.7	5.9±3.5	0.017
E_{cc} Apex, %	10.1±6.5	10.9±7.4	0.689
E_{cc} Mid, %	10.3±6.8	10.7±6.6	0.828
E_{cc} Base, %	8.2±6.8	11.4±4.8	0.064
LV longitudinal strain, %	10.8±7.3	11.3±7.5	0.837
LV longitudinal strain rate, %/s	54.2±37.1	59.7±44.2	0.629

Data as mean ± SD or n (%). E_{cc}, Circumferential strain. LGE, Late gadolinium enhancement. LVEDV, left ventricular end diastolic volume. LVEDVi, left ventricular end diastolic volume indexed to body surface area. LVEF, left ventricle ejection fraction. LVESV, left ventricular end systolic volume. LVM, left ventricular mass. LVMi left ventricular mass indexed.
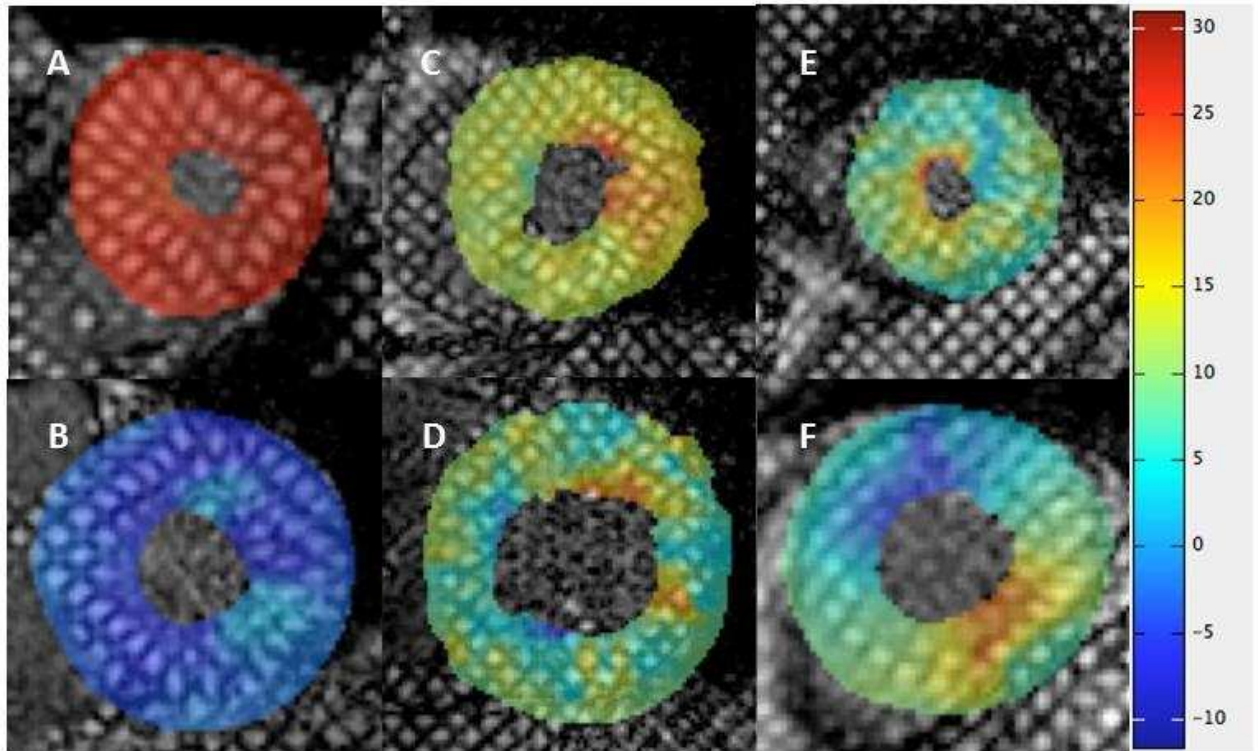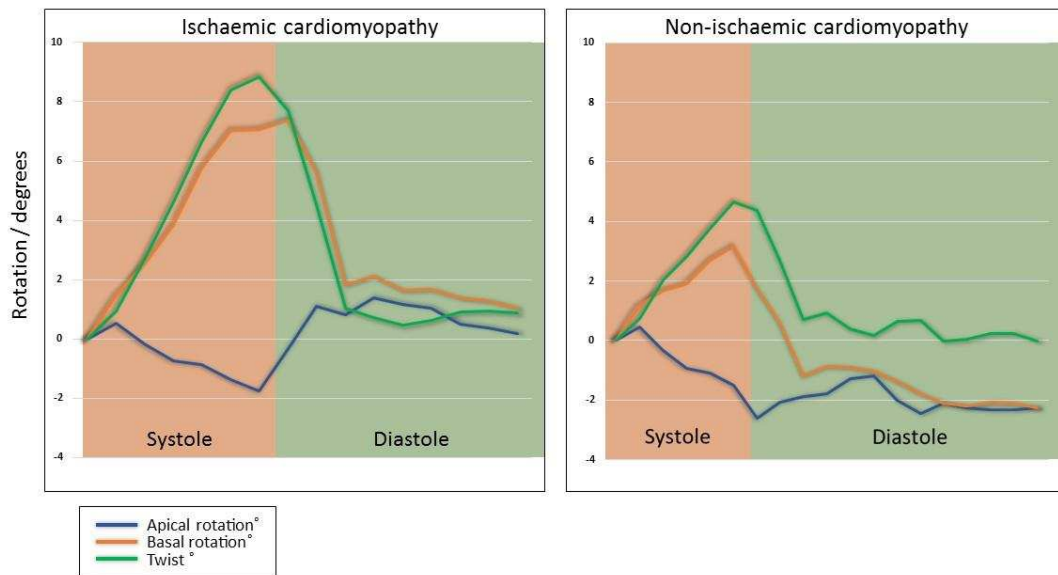
Figure 1.

Figure 2.

Figure 3.

A — LV Torsion

B — Ischaemic cardiomyopathy

C — Non-ischaemic cardiomyopathy